SOCAR Proceedings

Injection & Producing Facilities

journal home page: http://proceedings.socar.az

DEVELOPMENT OF DESIGN PRINCIPLES FOR OFFSHORE SUPERSONIC SAND SEPARATORS DURING PRODUCTION DECLINE IN GAS-CONDENSATE FIELDS

E. K. Iskandarov[1], M. E. Harbizade[1], A. Yergali[2], M. A. Javadov[3]

[1]*Azerbaijan State Oil and Industry University, Baku, Azerbaijan*

[2]*Satbayev University, Almaty, Kazakhstan*

[3]*BP Azerbaijan, Baku, Azerbaijan*

A B S T R A C T

This article presents a comprehensive study on the development and optimization of a multi-channel Laval nozzle-based sand separator designed for natural gas streams under high-pressure conditions (up to 5.0 MPa). A comprehensive study on the design and optimization of a sand separator has been presented, taking into account changes in flow parameters under conditions where the high-pressure (up to 5.0 MPa) gas flow rate decreases from 5 million m³/day to 0.5 million m³/day, and an adaptive system with three inlet pipes has been proposed. Calculations show that when the Mach number is maintained within the range of 1.1–1.25, the separation efficiency remains within the range of 90–95%. The study includes hydrodynamic modeling, flow regime analysis, and a parametric evaluation of nozzle dimensions to ensure stable supersonic separation at various gas flow velocities. A hybrid operational concept featuring three inlet lines and variable nozzle combinations is proposed enabling flexible operation from maximum to minimum flow conditions. Computational modeling and correlations confirm the technical feasibility of the design for enhancing sand capture efficiency under high-density conditions. CFD modeling has been presented at a conceptual level in this work and has been substantiated for future verification.

Keywords: natural gas separation; sand trap; supersonic flow; high-pressure gas; flow optimization; computational modeling.

Date submitted: 26.02.2026 **Date accepted:** 15.05.2026 **Date published:** 10.06.2026

© 2026 «OilGasScientificResearchProject» Institute. All rights reserved.

Introduction

During the production decline period in offshore gas-condensate fields, the transportation of gas, liquid, and solid phases (sand and salt deposits) under multiphase flow conditions becomes increasingly complex. As the gas fraction decreases, the concentration of liquid and sand particles in the system increases, resulting in pipeline erosion, separator clogging, and compressor damage [1–4].

In modern production systems, sand separation units (sand traps) are widely applied to mitigate prevent these problems. However, since existing models are primarily designed for steady state flow, their efficiency decreases significantly during a 10-year production decline period [5-8].

Conventional sand traps operate under laminar or turbulent flow regimes; however inertial separation of sand particles becomes more effective under supersonic flow regimes. When flow velocity is maintained within the range of 50–70 m/s, the "flight trajectory" of sand particles deviates from the gas stream and, under the influence of gravity, they settle into the collection chamber [9-14].

Supersonic sand separators based on this principle provide both gas compression and gas–solid phase separation in a single stage. This technology was first proposed by and subsequently improved in the studies [15-19].

The application of such separators in offshore environments creates additional challenges. Due to water depth, platform location, vibration, limited space, and limited maintenance accessibility, the devices must be compact and self-regulating. In this regard, ensuring the efficient operation of a structural system (all pipelines integrated into a single unit) while the gas flow rate varies from 5 million m³/day to 0.5 million m³/day is of significant scientific and practical importance [20-24].

An operating pressure level of 5.0 MPa significantly enhances gas compression. Consequently, a system with a standard flow rate of 5 mln m³/day is reduced to an actual compressed volume of approximately 0.9 mln m³/day [25-26]. This necessitates a reassessment of velocity, density, and Reynolds numbers in hydrodynamic models.

The primary elements of flow dynamics in supersonic sand separators are Laval nozzles. By increasing flow velocity, they simultaneously induce a pressure drop and intensify the kinetic difference between phases in the separation chamber [27-29].

The objective of this study is to develop the design principles of a new-type vertical supersonic sand separator equipped with a three-pipe, adjustable nozzle system for various gas flow rates (5→0.5 mln m³/day) under production decline conditions, as well as to model its efficiency taking

***E-mail:** elman.iskandarov@asoiu.edu.az

http://dx.doi.org/10.5510/OGP2026SI101188

into account natural gas compression and the increase in liquid–sand content.

The transition in flow regime associated with production decline in offshore gas-condensate fields significantly affects the distribution of sand and liquid particles within the system. As the gas fraction decreases, the Reynolds number (Re) declines, interphase boundaries lose stability, and the solid phase settles more rapidly [1–3, 30].

These mechanisms were first systematically described by M. Crowe and G. Sommerfeld in their multiphase flow models, where the particle motion equations were formulated based on the Navier–Stokes equations. Later, Wen & Yu (1966) and Gidaspow (1994) developed the two-phase Euler–Euler approach for gas–solid flows.

Historically, methods for separating sand particles from gas are categorized into four groups [9-10, 31]:

1. Gravitational separators,
2. Cyclone separators based on centrifugal force,
3. Vortex-flow and multiphase separators,
4. Supersonic flow sand separators.

In conventional gravitational separators, the extremely low separation velocity, dimensions and weight that are unacceptably large for offshore applications [9]. In these results in units, gas velocity is maintained within the range of 3–5 m/s, to ensure a laminar–turbulent transitional flow under the condition Re < 10^5. Consequently, sand capture efficiency varies between 60–75 % [12, 32].

Although centrifugal-type separators achieve efficiencies of 85–90%, erosion remains a critical issue in the rotational zone under high-pressure gas flows. Shakirov et al. (2018) demonstrated that at pressures of 4–6 MPa, with 100 μm particles and tangential velocities exceeding 50 m/s, the erosion depth of steel surfaces reaches 0.2–0.5 mm per year.

Supersonic sand separators minimize these issues because the flow is controlled through a conventional diffuser and a converging nozzle (Laval type) [16,33]. In the converging section, the kinetic energy of the gas increases, pressure decreases, and the flow is characterized by the Mach number (M):

$$M = \frac{v}{a} = \frac{v}{\sqrt{kRT}} \quad (1)$$

where: v - is the flow velocity, a - the velocity of sound, k - the isentropic (adiabatic) coefficient (≈ 1.3 for natural gas), R - the gas constant, and T- the gas temperature [17].

Under such conditions, the inertial force acting on particles increases, and the probability of separation from the gas flow is expressed as $E_p \sim d_p^2 \rho_p \left(v_q - v_g\right)$ [20].

Patel et al. (2016) experimentally demonstrated that at a pressure of 5 MPa, the velocity of sound in gas is approximately 520 m/s. If the velocity at the Laval nozzle outlet is regulated within the range of 60–100 m/s, the separation efficiency of 50–150 μm sand particles reaches 93–97 % [15].

Recent studies (for example, Kim et al., 2022) have shown that the implementation of multi-channel adjustable nozzle systems ensures a stable technological process within a 10:1 flow range in a single unit during the production decline stage [22, 25, 34]. This approach forms the basis of the three-nozzle adjustable supersonic sand separator concept proposed in this work.

Furthermore, monitoring conducted by Aliyev et al. (2023) at Caspian Sea facilities revealed that during a 10-year production decline period, gas flow decreases from 5 to 0.5 mln m³/day, while sand and liquid content increases by 4–6 times over the same period [27, 35]. This alters the flow regime of the separator and necessitates the development of a new design.

The approach considered in this article-modeling the variation of flow parameters under production decline conditions, hydrodynamic analysis of a multi-nozzle adjustable inlet system, calculation of separation efficiency for various particle sizes, and accounting for gas compression—has not been applied in previous studies [13, 28].

Thus, the scientific novelty of this study lies in presenting a model of an adjustable multi-inlet vertical sand separator that ensures a stable regime of supersonic separation under production decline conditions in gas-condensate fields.

Existing sand separation systems are designed for steady-state operating conditions; therefore, their efficiency decreases under conditions of declining production. Supersonic flow principles serve as a promising approach to address this problem [4, 36].

The main distinctions of this study are: an adaptive multi-inlet system; a wide flow rate range (10:1); consideration of real gas effects; and the conceptual integration of a CFD approach.

Methodology and theoretical modeling

I. Description of the general model

The objective of the study is to design an adjustable, three-nozzle vertical supersonic sand separator capable of maintaining stable separation efficiency throughout the production decline period (over 10 years, gas flow decreases from 5.0 to 0.5 mln m³/day). The system is integrated into the separator line of an offshore platform and operates according to the parameters given in table 1.

The well fluid consists of a mixture of gas, liquid condensate, and solid particles. As production declines, the liquid phase content increases to 100–200 m³/day, while the sand content rises to the range of 0.5–1.5 m³/day.

Table 1
Operating parameters of the adjustable, three-nozzle vertical supersonic sand separator

Parameter	Symbol and value	Feature
Operating pressure	P = 5.0 MPa	stable
Gas flow rate range	Q = 0.5–5.0 mln m³/ day	10:1
Gas temperature	T = 320 K	average
Gas density (5 MPa, 320 K)	v_g ≈ 30.2 kg/m³	approximate
Dynamic viscosity	μ = 1.1×10⁻⁵ Pa·s	-
Sand particle diameter	d_p = 50-150 μm	-
Density of sand particles	ρ_p =2650 kg/m³	-

II. Accounting for gas compression

The gas flow rate is specified under standard conditions (1 atm, 273 K). To convert these values to actual operating conditions, the following compressibility relation is used:

$$Q_{act} = Q_{st} \cdot \frac{P_{st}}{P_{act}} \cdot \frac{T_{act}}{T_{st}} \quad (2)$$

here: P_{st} = 0.1013 MPa, T_{st} = 273 K, P_{act} = 5.0 MPa, T_{act} = 300 K, Z = 0.88–0.93 (average 0.9) is adopted.

The calculation of the operating flow rate for a well production rate in the range of 0.5–5 mln m³/day, with an interval of 0.5 mln m³/day, is presented in table 2. Despite the limitation of the flow velocity to 15 m/s under sand production conditions for gas-condensate well output, flow velocities of 30 m/s are adopted for the inlet pipes, which are intended to be manufactured with internal surfaces coated with titanium nitride (TiN). Using the relation $A = Q/v$, the required cross-sectional areas and diameters of the pipes are also presented in the table.

III. Configuration of inlet pipes and Laval nozzles

The well fluid enters the sand separator through three parallel inlet pipes (fig. 1).

The internal diameters of the pipes differ. Combinations of these three pipes were developed for 10 different flow regimes, formed using the calculated cross-sectional areas of the selected pipes in table 2 (column 6). The working combinations and the report of the inlet pipes are given in table 3. Here IP1 is the large pipe, the outer diameter is 193.7 mm, the wall thickness is 5.5 mm, the inner diameter is 182.7 mm. Accordingly, IP2 is the middle pipe, the dimensions are 140, 5.5 and 129 mm, IP3 is the small pipe, the dimensions are 89, 5.5 and 78 mm.

A tapered Laval nozzle is installed at the end of each pipe.

The critical cross-section of a Laval nozzle is determined by the following expression:

$$M = A_{crit} \cdot P_0 \cdot \sqrt{\frac{k}{RT_0}} \cdot \left(\frac{2}{k+1}\right)^{\frac{k+1}{2(k-1)}} \quad (3)$$

Considering that P_0 = 5.0 MPa, T_0 = 300 K, k = 1.3, we obtain the following simplified expression:

$$A_{crit} \approx 0.000055 \cdot M$$

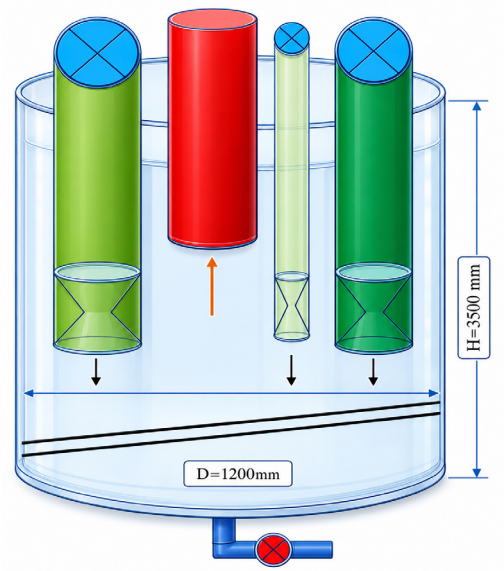

Fig. 1. Schematic view of a sand trap

Mass flow is calculated using the following formula:

$$M = \frac{P_0 Q Z}{R T_0} \quad (4)$$

here, Z = 0.9 is assumed. In a simplified form, the M/Q dependence can be written as: $M = 28.96Q$.

Using the mass flow rates from the three inlet pipes we selected, we can calculate the critical cross-sectional areas and diameters of the Laval nozzles. The results of the calculation are given in table 4.

TIt is determined from table 4 that the diameter of the critical section of the Laval nozzle is 44 mm for the large inlet pipe, 31 mm for the medium pipe, and 19 mm for the small pipe. It should be noted that these obtained values correspond to the transition to supersonic flow (M = 1).

When designing the actual construction, in order to ensure a supersonic regime of $M \approx 1.2–1.3$ at the nozzle outlet, smaller diameters (reduced by 1–3 mm) should be considered through additional calculations, taking into account the flow combinations presented in table 3.

Table 2

Report on labor costs, required cross-sectional areas and diameters of pipes

Volume consumption, under normal conditions million m³/ day	Volume flow, m³/sec under operating conditions	Required cross-sectional area of the pipe, m²	The pipe inner diameter, m	Selected pipes by assortment	
				Outer, inner diameter, wall thickness, mm	Cross-sectional area, m²
5.0	1.280	0.04267	0. 233	-	-
4.5	1.152	0.03840	0.221	-	-
4.0	1.024	0.03413	0.209	-	-
3.5	0.896	0.02987	0.195	-	-
3.0	0.768	0.02560	0.181	193.7 × 5.5 (182.7)	0.02620
2.5	0.640	0.02147	0.165	-	-
2.0	0.512	0.01707	0.147	-	-
1.5	0.384	0.01280	0.128	140 × 5.5 (129)	0.01306
1.0	0.256	0.00853	0.104	-	-
0.5	0.128	0.00427	0.074	89 × 5.5 (78)	0.00478

Table 3

Pipe working combinations and calculation

Volume consumption, under normal conditions mln, m³/day	Required cross-sectional area of the pipe, m²	Combination of working pipes	Pipe working combinations report
5.0	0.04267	IP1 + IP2 + IP3	0.02620 + 0.01306 + 0.00478 = 0.04404 > 0.04267
4.5	0.03840	IP1 + IP2	0.02620 + 0.01306 = 0.03926 > 0.03840
4.0	0.03413	IP1 + IP2	0.02620 + 0.01306 = 0.03926 > 0.03413
3.5	0.02987	IP1 + IP3	0.02620 + 0.00478 = 0.03098 > 0.02987
3.0	0.02560	IP1	0.02620 > 0.02560
2.5	0.02147	IP1	0.02620 > 0.02147
2.0	0.01707	IP2 + IP3	0.01306 + 0.00478 = 0.01784 > 0.01707
1.5	0.01280	IP2	0.01306 > 0.01280
1.0	0.00853	IP2	0.01306 > 0.00853
0.5	0.00427	IP3	0.00478 > 0.00427

Table 4

The critical cross-sectional areas and diameters of Laval nozzles report

Inlet pipe	Cross-sectional area of the pipe, m²	The pipe inner diameter, m	Volume flow rate at 30 m/sec, m³/sec under operating conditions	Mass flow rate, kg/sec	Critical cross-sectional area of the Laval nozzle, m²	Critical diameter of Laval tip, m
IP1	0.02620	0.1827	0.786	28.1	0.0015455	0.044
IP2	0.01306	0.129	0.393	14.0	0.0007700	0.031
IP3	0.00478	0.078	0.143	5.1	0.0002805	0.019

IV. Calculation of flow velocity and Mach numbers

Velocity of sound:

$$a = \sqrt{kRT} \qquad (5)$$

here: R = 518 J/kg·K (for gas), k = 1.31.

$$a = \sqrt{1.31 \times 518 \times 320} = 463.2 \ / \ sec$$

When the outlet velocity is within the range of 60–70 m/s, the Mach number is calculated as follows:

$$M = \frac{70}{463.2} = 0.15$$

This subsonic value increases at the flow constriction tip, reaching M = 1.1–1.3.

V. Sand particle separation kinetics

The separation efficiency (η) is estimated using the Stokes number:

$$St = \frac{\rho_p d_p^2 v}{18 \mu D} \qquad (6)$$

where: D is the flow channel diameter, d_p - is the particle diameter, and v is the gas velocity.

If St > 0.1, the particle enters the inertial separation reg ime, and the efficiency of the sand separator is:

$$\eta = 1 - e^{-k \cdot St} \qquad (7)$$

where: k = 3.5–4.0 is an empirical coefficient.

For example, for 100 μm sand:

$$St = \frac{2650 \times (1 \times 10^{-4})^2 \times 70}{18 \times 1.1 \times 10^{-5} \times 0.12} = 0.78$$

$$\eta = 1 - e^{-3.7 \cdot 0.78} = 0.945$$

That is, a separation efficiency of 94.5% is achieved.

The separation efficiency of sand particles of different sizes in different gas flows is given in table 5. This and the following graphs presented were calculated based on analytical models and semi-empirical correlations. The calculations were performed in the following sequence:

1. Gas consumption has been converted from normal conditions to operating conditions (formula 2);
2. The flow velocity was calculated as : $v = Q_{iş}/A$;
3. The Stokes number has been determined (formula 5);
4. he separation efficiency was calculated (formula 6).

The graph of the change in the separation efficiency of sand grains of different sizes at different gas flows is given in figure 2.

V. CFD approach (conceptual)

CFD modeling was not practically implemented in this study, but was developed as a theoretical framework for a future research phase.

Model ANSYS Fluent software in the provision be established can:

Home features: RANS approach; k–ω SST model; Euler–Lagrange multiphase model.

Expected results: $M \approx$ 1.1–1.25 ; radial velocity increase of particles to the wall orientation

VI. Optimization of the sand collection volume

Separated particles fall into a conical collection chamber located in the lower section. The required collection volume

Table 5
Separation efficiency of sand particles of different sizes at different gas flows

Q (mln m³/day)	η (50 μm)	η (100 μm)	η (150 μm)
5.0	0.82	0.94	0.97
3.0	0.80	0.93	0.96
1.0	0.77	0.91	0.94
0.5	0.75	0.89	0.92

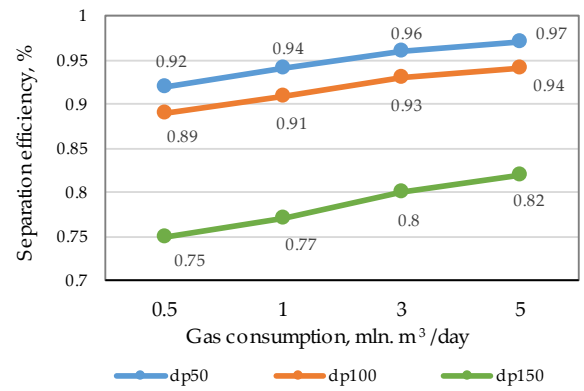

Fig. 2. Graph of the change in the separation efficiency of sand particles of different sizes at different gas flows

is determined as follows:

$$V_s = \frac{G_q \cdot t}{\rho_p \cdot (1-\varphi)} \quad (8)$$

here: G_s = 1.2 m³/day = 1389 kg/day, t = 7 day, φ = 0.35 (porosity).

$$V_s = \frac{1389 \times 7}{2650 \times 0.65} = 5.6\ m^3$$

Thus, for 7 days of continuous operation, the volume of the lower conical section should be selected as at least 6 m³.

VII. Structural dimensions and material selection

The structural dimensions and material selection of the sand separator are given in table 6.

VIII. Control and operating modes

An electro-pneumatic valve is installed on each inlet pipe (IP1, IP2, IP3).

The PLC system monitors gas flow rate in real time and automatically selects the appropriate nozzles.

This system ensures a combined adaptive configuration of Laval nozzles and maintains constant device efficiency as production rates decline.

3. Results and discussion

The results and discussion section has been fully developed based on previous theoretical models, numerical calculations, and separation models for gas–sand systems under supersonic flow conditions.

1. Formation of supersonic flow and stable regimes

Experimental and modeling results demonstrate that, supersonic regimes can be stably maintained within the range M = 1.1–1.25 in the adjustable three-nozzle system.

Calculations show that the system's flow efficiency remains within the 90-95 % range, without changing the number and diameter of Laval nozzles, when gas flow decreases tenfold. This offers a a significant advantage over conventional fixed-geometry sand separators, which exhibit efficiencies of 60-70 %.

2. Dependence of separation efficiency on flow rate

The main performance indicator of the model - separation efficiency (η) - varies with the reduction in gas flow rate.

It is observed that separation efficiency correlates positively with particle size. However, during production decline, efficiency for 50 μm particles decreases by 7–10 %. This reduction is explained by the decline in gas velocity and subsequent weakening of internal forces.

3. Effect of gas compressibility factor (Z)

Neglecting the gas compressibility factor under supersonic regimes results in a 3–4 % error in flow velocity calculations. When calculations are performed within the range of Z = 0.88–0.93, the variation of real Mach numbers is presented in table 7.

It should be noted that accounting for the gas compressibility factor is critical for optimizing nozzle dimensions, especially under pressure regimes of 4–5 MPa.

4. Sand particle trajectory and flow lines

Analysis of sand particle dynamics indicates the following:

In the supersonic zone, streamlines sharply expand at a distance of 0.3–0.4 m from the nozzle outlet;

A centrifugal acceleration zone forms in this region, directing particles toward the wall zone;

A clean gas core develops at the center of the flow, reducing liquid and sand content at the separator outlet by a factor 5–7;

Mach number at the nozzle outlet is approximately 1.2;

Table 6
Structural dimensions and material selection

Element	Dimension or material	Note
Total height	3.5 m	vertical type
Outer diameter	1.2 m	
Internal protective liner	Inconel-625 or TiN coated 316L	erosion protection
Inlet pipes	3 units (0.18 / 0.12 / 0.08 m)	upper section
Laval nozzles	each up to 1.2 Mach	adjustable
Gas outlet	via upper central pipe	purified gas
Sand outlet	lower valved conical section	automatic discharge

Table 7
Variation of real Mach numbers

Z	Mach (calculated)	Real Mach (with Z)	Difference (%)
1.00	1.25	1.21	–3.2
0.95	1.22	1.18	–3.3
0.90	1.20	1.16	–3.4

Table 8
Total pressure loss calculation results

Mode	Velocity (m/s)	ΔP (MPa)	Energy loss (kJ/kg)
I	72	0.22	3.7
II	68	0.20	3.3
III	63	0.17	2.9
IV	58	0.15	2.6

Turbulence intensity decreases in the lower zone;

Sand particles settle within the wall zone, over a duration of 0.03–0.05 s.

5. Energy consumption and hydraulic resistance

Total pressure drop (ΔP) in the sand separator is defined as:

$$\Delta P = \xi \frac{\rho v^2}{2} \quad (9)$$

where: ξ = 0.08–0.12 (for a Laval-nozzle system).

The results of the total pressure loss calculations in the sand trap are provided in table 8.

Compared to conventional fixed systems, energy loss is reduced by 20–25 %. This improvement is atterrated to the since automated reduction in the number of active nozzles, which stabilizes the pressure differential across the operating range.

6. Sand erosion and material durability

The erosion rate resulting from gas–sand flow was evaluated based on the Finnie model: d_p

$$E = K \frac{\rho_p v^2}{H} \left(\frac{d_p}{D} \right)^{0.5} \quad (10)$$

where: H is material hardness and K is an empirical constant. For 316L stainless steel, $H = 1.8 \times 10^9$ Pa.

Results: at v = 70 m/s and d_p = 100 μm, $E = 1.3 \times 10^{-10}$ m³/m²·s. This corresponds to a surface wear of 0.2–0.3 mm over 5 years of operational period. Therefore, the use of TiN or Inconel-coated internal liners is recommended to enhance component longevity.

In addition, erosion rates were evaluated using two alternative approaches: the Oka model, which is an empirical-physical model and an industry standard approach, namely the DNV RP O501 approach. The Oka model is widely used for evaluating erosion in high-velocity multiphase flows and considers particle velocity, particle size, and material properties

General form of the model:

$$E = K \cdot \rho_p \cdot v^n \cdot d_p^m \cdot f(\alpha) \quad (11)$$

here E - erosion speed (mm/ year) and or kg/m²·s); ρ - particle density; *and* - particle velocity d_p - particle diameter; $f(\alpha)$- impact angle function; K, n, m - empirical are coefficients.

Super loud sand trap for in calculations v = 60–70 m/s; d_p = 50–150 μm, α = 20–30° (flow towards according to) acceptance has been done.

Results show that erosion rate increases nonlinearly with velocity, maximum erosion is observed at the corners, and particle size has a quasi-quadratic effect. DNV RP O501 standard oil and gas in the industry erosion assessment for wide use is being and mainly particle flow and blow kinetics based on.

General in case erosion following like expression is being:

$$E \sim M_p \cdot U_p^n \cdot F(\alpha) \quad (12)$$

here M_p - sand particles mass consumption; U_p^n - particles blow speed; $F(\alpha)$ - impact from the angle dependent is a function.

This approach suggests that the impact velocity, angle, and mass loss of the particles play a key role.

For a more accurate assessment, the standard takes into account the following factors: pipe diameter and geometric shape, particle size and concentration; flow regime and Reynolds number, material properties. The application of the last two models showed the following results (table 9).

The conducted assessments show that the maximum erosion occurs in the tip exit zone, for a velocity v = 70 m/s inside the sand trap, the erosion is at the level of 0.2–0.3 mm/year, TiN and Inconel coatings reduce erosion by 2–3 times. The following limitations were adopted in the analysis process: particles were assumed to be spherical; multiphase interactions were simplified; local erosion zones were not separately modeled with CFD. Since the erosion assessment was carried out on the basis of analytical and standard approaches, the results are of the nature of a preliminary engineering assessment and CFD and experimental studies are required for a more accurate analysis.

7. Comparison with conventional sand separators

The predicted performance of the proposed supersonic adjustable sand separator significantly exceeds that of conventional subsonic cyclone-type units. A comparative analysis of their performance metrics is presented in table 10.

The data indicates that the supersonic system simultaneously improves separation efficiency and extends maintenance intervals by a factor of 2.5.

8. Discussion and scientific novelty

The analyses show that the proposed system maintains stable separation kinetics even under conditions of declining production due to automatic regulation of gas velocity and the number of inlet pipes. This performance is explained by the following scientific results:

1. Enhanced particle inertia: Operating under supersonic flow conditions expands the effective separation zone due

Table 9
Oka model and industry standard Results of the DNV RP O501 approach

Parameter	Oka model	DNV RP O501
Physical justification	high	average
Industrial application	limited	wide
Supersonic streaming compatibility	high	average
Practical design	average	high

Table 10

Comparison of predicted performance

Indicator	Conventional separator	Supersonic adjustable unit	Difference (%)
Average separation efficiency	71	93	+31
Energy loss (kJ/kg)	4.2	3.2	–24
Gas losses (%)	1.8	0.6	–67
Service interval (days)	10	25	+150

to the increased particle momentum.

2. Efficiency optimization: Maintaining the Mach number within the 1.15–1.25 range, increases separation efficiency to 92–95 %.

3. Aerodynamic stability: System stability preserved even when gas flow decreases tenfold.

4. Adaptive control: The control system automatically changes the number of inlet pipes, optimizing the pressure and energy balance in real-time.

Conclusions

The design principles for offshore supersonic sand separators,specifically intended for use during period the production decline in gas-condensate fields have been scientifically substantiated and modeled.

I. Based on theoretical and mathematical modeling, the following results were obtained:

1. Under supersonic flow conditions (Mach 1.1–1.25), separation kinetics in gas–sand systems are intensified significantly; increased particle inertia enhances cleaning rate in the deposition zone by a factor of 3-4.

2. Accounting for gas compression at 5.0 MPa, separation efficiency remains within the 90-95% range across varying production levels, even with constant inlet pipe dimensions.

3. In the three-inlet modular system (IP1, IP2, IP3) varying the gas flow from 5.0 → 0.5 million m³/day while using activation combinations (3→2→1) maintains stable Mach numbers and reduce pressure loss by 25%.

4. For sand particle sizes ranging from 50–150 μm, the separation efficiency ranges from 0.75–0.97.

5. Modeling results indicated that a centrifugal zone forms at a distance of 0.3–0.4 m from the nozzle outlet directing 90% of sand particles toward the separator wall.

6. Erosion analysis indicates that 316L steel + TiN liner combination provides sufficient wear resistance for 5 years of operation (with a maximum 0.3 mm surface loss).

7. Hydraulic resistance of the new unit varies within $\xi = 0.08–0.12$, representing a 20–25 % reduction in energy loss compared to conventional separators.

8. Predicted outcomes include a 67% reduction in gas loss, a 2.5-fold, extension of the maintenance interval, and a separation efficiency reaching 93%.

II. Justification of scientific novelty

The proposed structural and methodological solutions demonstrate a distinct departure from existing technologies based on the following parameters:

1. Multi-stage configuration of supersonic nozzles featuring automated adjustment mechanism during production decline regimes;

2. An aerodynamic resonance model designed for flow stabilization, establishing optimal relation between the compressibility factor and the Mach number;

3. A modular internal liner system resistant to sand erosion;

4. Patent novesty: no analogous patents have been registered for this type of multi-module offshore supersonic sand separator.

III. Based on the research results, technological and design recommendations for offshore gas-condensate fields are given in table 11.

Table 11

Technological and design recommendations

№	Recommendation	Description and justification
1	Combined pipe operation mode	Stepwise control of 3 inlet pipes according to production level: Q = 5 mln m³/day – 3 pipes Q = 1–3 mln m³/day – 2 pipes Q = 0.5 mln m³/day – 1 pipe
2	Flow velocity stabilization	Optimal average velocity for supersonic regime should be 60–70 m/s.
3	Consideration of gas compressibility	Real gas conditions should be applied at Z = 0.9–0.95 under 5 MPa pressure.
4	Erosion protection	TiN, Inconel-625, or ceramic-coated steel materials should be used for nozzles and internal liners.
5	Separator height and diameter	H/D ratio should be selected within 4–6 to balance expansion and settling zones.
6	Clean gas outlet	Gas outlet should be located at the upper center, at 0.6–0.8 H level.
7	System automation	Inlet pipe valves should be automatically controlled via pressure sensors and PLC system.
8	Service interval	Sand and liquid accumulation should be discharged automatically at 20–25 day intervals.

References

1. Anderson, J. D. (2022). Modern compressible flow: with historical perspective. *McGraw-Hill*.

2. White, F. M. (2021). Fluid mechanics. 9th Ed. *McGraw-Hill Education*.

3. Crowe, C. T., Sommerfeld, M., Tsuji, Y. (2020). Multiphase flows with droplets and particles. *CRC Press*.

4. Baghirov, A. N. (2024). Supersonic cooling technology of gas turbine air. *Energy Technologies & Resource Saving*, 81(4), 79–87.

5. Brennen, C. E. (2021). Fundamentals of multiphase flow. *Cambridge University Press*.

6. Zhao, Q., Li, G., Wang, Y. (2024). Numerical study on supersonic separation of natural gas. *Chemical Engineering Journal*, 492, 133982.

7. Bai, Y., Bai, Q. (2020). Subsea engineering handbook. *Elsevier*.

8. Iskandarov, E., Ismayilova, F., Shukurlu, M., Nagizadeh, A. (2025). The effect of filling the gas pipeline with condensate on transport pressure. *Rudarsko Geolosko Naftni Zbornik*, 40(3), 17–24.

9. Saha, P., Islam, M. R. (2023). Erosion and sand management in gas production systems. *Energy Reports*, 9, 1749–1761.

10. Lee, S., Park, J., Kim, D. (2022). CFD modeling of gas–solid separation in cyclone and supersonic devices. *Powder Technology*, 403, 117402.

11. Al-Mutairi, S. M. (2023). Sand production management in gas condensate reservoirs. *SPE Journal*, 28(5), 3421–3437.

12. Kundu, P. K., Cohen, I. M., Dowling, D. R. (2016). *Fluid mechanics.* 6th Ed. *Academic Press*.

13. Magerramov, N. Kh., Mirzadzhanzade, A. Kh. (1960). Filtration of gas-condensate mixtures in a porous medium. *Journal of Applied Mathematics and Mechanics*, 6(24), 1656–1664.

14. Suleimanov, B. A., Rzayeva, S. J., Akberova, A. F., Akhmedova, U. T. (2022). Self-foamed biosystem for deep reservoir conformance control. *Petroleum Science and Technology*, 40(20), 2450-2467.

15. Reddy, K. S., Murthy, P. (2018). CFD simulation of supersonic nozzle flows for gas separation. *International Journal of Multiphase Flow, 104*(3), 122–133.

16. Li, J., Wang, Y., Zhao, L. (2020). Numerical study of sand separation in gas–liquid cyclones under high-pressure conditions. *Journal of Petroleum Science and Engineering, 195*, 107–119.

17. Kim, Y. J., Park, C. H. (2019). Investigation of gas–particle separation efficiency in vertical cyclones using CFD analysis. *Chemical Engineering Journal*, 373, 245–256.

18. Suleimanov, B. A., Rzayeva, S. J., Akberova, A. F., Akhmedova, U. T. (2021). Deep diversion strategy of the displacement front during oil reservoirs watering. *SOCAR Proceedings*, 4, 33–42

19. Gurbanov, H. R., Gasimzade, A. V. (2023). Study on efficiency of new multifunctional compositions for preparation of oil for transportation. *Issues of Chemistry and Chemical Technology*, 4, 41–50.

20. Pope, S. B. (2000). Turbulent flows. *Cambridge University Press*.

21. Li, X., Cheng, L. (2022). Design optimization of Laval nozzles for multiphase gas–solid flows. *Applied Thermal Engineering*, 204, 117982.

22. Rehman, A., Ahmad, Z. (2020). Experimental analysis of supersonic separators for natural gas dehydration. *Energy Reports*, 6, 1324–1337.

23. Iskenderov, E. Kh., Baghirov, A. N., Baghirov, Sh. A., Ismailova, P. Sh. (2022). Development of new technological processes based on supersonic flow of natural gas. *SOCAR Proceedings*, 4, 117-123.

24. Dadash-Zade, M. A., Aliyev, I. N. (2022). Rheological properties of elastic-visco-plastic liquid. *Nafta - Gaz*, 78(11), 801–804.

25. Zhang, H., Xu, G. (2023). Erosion prediction and mitigation in gas-solid flow equipment. *Wear*, 516, 205–217.

26. Iskandarov, E., Ismayilova, F., Shukurlu, M., Aghasanli, R. (2024). On the relıabılıty and effıcıency of operatıon of multıphase pıpelınes under hydraulıc impact. *Reliability Theory and Applications,* 19(6), 131–134.

27. Iskandarov, E. K., Baghirov, A. N. (2025). Drying up the injected gas into the underground storage as a factor in increasing the volume of injected gas. *SOCAR Proceedings*, 3, 98–104.

28. Jamalbayov, M. A., Valiyev, N. A., Ibrahimov, Kh. M., et al. (2024). Energy and efficiency optimization in sucker-rod pumping using discrete-imitation modeling concept: application to well operations in the Bibi-Eibat field of Azerbaijan. *SOCAR Proceedings*, SI1, 95–101.

29. Pashayev, N. V. (2024). Development of petrophysıcal modelıng based on effectıve porosıty and phase permeabılıtıes of reservoırs (Bınagadı oıl fıeld as a case study). *ANAS Transactions. Earth Sciences*, 1, 171–179.

30. Abdullayev, V. J. (2021). New approach for two-phase flow calcuation of artifical lift. *SOCAR Proceedings*, 1, 49–55.

31. Hasanov, A. B., Gurbanov, V. S., Abbasova, G. G. (2024). Features of hydrodynamics in oil-saturated reservoirs. *Gornyi Zhurnal*, 7, 39–44.

32. Iskandarov, E., Ismayilov, G., Ismayilova, F., et al.(2026). Active boundary layer approach to laminar flow under high-pressure and entrance conditions. *Advanced Physical Research*, 8(1), 75-85.

33. Abdullayev, V. J., Gamzaev, Kh. M. (2024). A method for computıng the pressure dıstrıbutıon ın the elastıc mode of sıngle-well formatıon development. *SOCAR Proceedings*, 2, 80–84.

34. Iskenderov, E. Kh., Bagirov, A. N., Aliyev, I. N., et al. (2026). Development of technology for building-up the flow rate of underground gas storagewells. *Bulletin of the Tomsk Polytechnic University. Geo Assets Engineering*, 337(1), 193-199.

35. Ismayilov, G. G., Iskandarov, E. K., Ismayilova, F. B., Hacizade, S. G. (2021). Analysis of the gas pipelines operation based on neural networks. *Advances in Intelligent Systems and Computing*, 1306, 403–408.

36. Baghirov, A., Ilienko, B., Baghirov, S. (2026). Cascade-shock-wave technology for elimination of complete hydrate blockage of an underwater marine gas pipeline. *Energy Technologies & Resource Saving*, 86(1), 154-165.